

New material of *Mongolemys elegans* Khosatzky and Mlynarski, 1971 (Testudines: Lindholmemydidae), from the Late Cretaceous of Mongolia with comments on bone histology and phylogeny

EDWIN A. CADENA¹, DANIEL T. KSEPKA^{1,2}, AND MARK A. NORELL³

ABSTRACT

Mongolemys elegans Khosatzky and Mlynarski, 1971, is a freshwater lindholmemydid turtle that is very abundant in Late Cretaceous (Maastrichtian) pond deposits from the Gobi Desert of Mongolia. Here, we present new data on the morphology, bone histology, and phylogenetic position of *M. elegans* based on hatchlings, juveniles, and adults collected by American Museum of Natural History and the Mongolian Academy of Sciences joint field expeditions at the Bugin Tsav locality. Phylogenetic analysis using a morphological dataset supports the placement of *M. elegans* as a stem testudinoid. Bone histology of *M. elegans* shows similar patterns of thickness and bone tissue type for the internal and external cortices as in other freshwater turtles. Microstructural samples of fossil bone from *M. elegans* show exceptional preservation of osteocyte lacuno-canicular networks, and higher values of osteocyte density at the external cortex in contrast to cancellous bone and the internal cortex.

INTRODUCTION

Cretaceous fossil turtles from Asia were diverse and occupied a wide range of habitats including terrestrial, fluvial, estuarine, and coastal plain environments (Brinkman et al., 1993;

¹ Department of Marine, Earth, and Atmospheric Sciences, North Carolina State University, Raleigh, North Carolina, 27695.

² Department of Paleontology, North Carolina Museum of Natural Sciences, Raleigh, North Carolina, 27601.

³ Division of Paleontology, American Museum of Natural History, New York, NY, 10024.

Danilov, 1999a, 1999b; Sukhanov, 2000; Danilov et al., 2002; Danilov and Parham, 2005). The extinct Lindholmemydidae comprises one of the most diverse Early Cretaceous-Paleocene radiations. This clade includes the genera *Tsaotanemys* from the ?Albian of China (Sukhanov, 2000); *Khodzhakulemys* from the upper Albian–lower Cenomanian of Uzbekistan (Danilov, 1999a); *Paragravemys* from the Cenomanian–early Turonian of Mongolia (Shukhanov et al., 1999); *Lindholmemyd* from the Turonian–early Campanian of Middle Asia and Kazakhstan (Danilov and Sukhanov, 2001); *Hongilemys* from the Turonian-Campanian of Mongolia (Sukhanov and Narmandakh, 2006), and three Maastrichtian genera: *Mongolemys* and *Gravemys* from Mongolia (Sukhanov, 2000; Danilov, 2003), and *Amuremys* from the Amur River (Russia-China border) (Danilov et al., 2002). Lindholmemydids are also represented by two Paleocene genera from China; *Hokouchelys* Yeh, (1994) and the recently redescribed *Elkemys* Danilov et al., (2012). Of all the taxa assigned to Lindholmemydidae, however, only *Mongolemys elegans* and *Lindholmemyd elegans* are known from shell and cranial material (Sukhanov, 2000; Danilov, 2004), and material is very fragmentary for *Lindholmemyd elegans*.

Mongolemys elegans was initially assigned to Dermatemydidae by Khosatzky and Mlynarski (1971) based on the similarities of this fossil to Central American river turtle *Dermatemys mawii* (Gray, 1847), the only extant representative of Dermatemydidae. These similarities include the presence of large inframarginal scales, epidermal sculpturing of the shell, alveolar surfaces of the jaw, strong development of the temporal region, strongly developed hyoidal elements, and a hooklike process in the maxilla and dentary. Later discoveries showed that the inframarginal scales are more likely a primitive feature retained by dermatemydids and lindholmemydids that these groups are only distantly related (Shuvalov and Chkhikvadze, 1975; Sukhanov, 2000; Danilov and Sukhanov, 2001). *Lindholmemyd* and *Mongolemys* have been considered to be close relatives of Testudinoidea (tortoises, pond turtles, and allies) (Danilov and Parham, 2005; Lourenco et al., 2012), though another large scale study noted that the phylogenetic placement of *Mongolemys* remains poorly understood (Joyce, 2007).

Despite of the abundant number of fossil specimens of lindholmemydids and their potential importance for the understanding of the emergence of Testudinoidea (the most diverse and widespread clade of extant and Cenozoic turtles), almost nothing is known about their bone histology or ontogenetic variation. Here, we describe new specimens of *Mongolemys elegans* collected by American Museum of Natural History (AMNH) and Mongolian Academy of Sciences joint field expeditions at the Bugin Tsav locality (fig. 1) including hatchlings, juveniles, and adults. We also present a description of bone macrostructure (cancellous and cortical bone) and microstructure (Harvesian systems, osteons, bone cells) with a focus on ontogenetic changes.

INSTITUTIONAL ABBREVIATIONS

AMNH	American Museum of Natural History, New York, NY
IGM	Geological Institute of the Mongolian Academy of Sciences, Ulaan Baatar, Mongolia
NCSM	North Carolina Museum of Natural Science (herpetology collection), Raleigh, NC

PCHP	Chelonian Research Institute, Peter C.H. Pritchard, Oviedo, FL
PIN	Paleontological Institute, Russian Academy of Sciences, Moscow, Russia
UF	University of Florida, Florida Museum of Natural History Vertebrate Paleontology Collections, Gainesville, FL
USNM	Smithsonian National Museum of Natural History, Washington D.C.
Z. Pal.	Paleozoological Institute, Polish Academy of Sciences, Warsaw, Poland
ZIN	Zoological Institute, Academy of Sciences, Leningrad, Russia

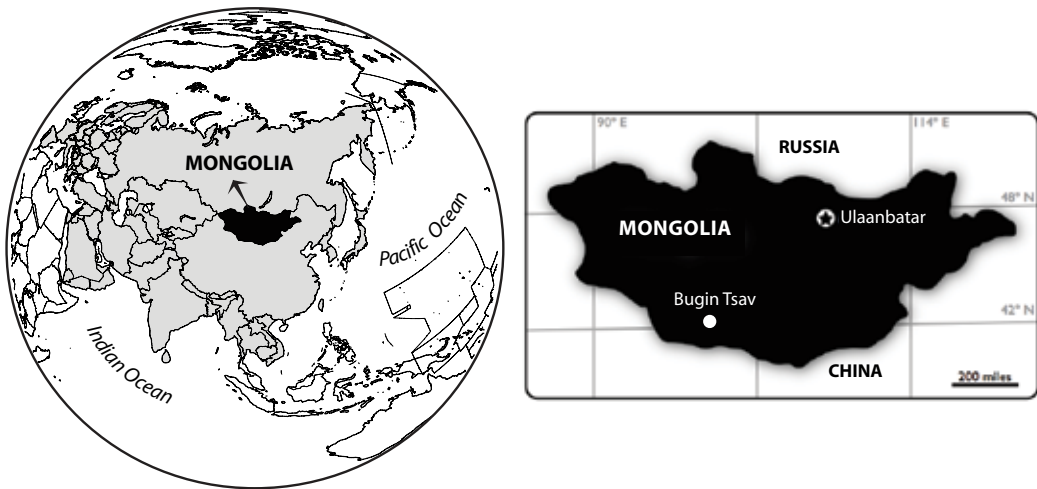


FIG. 1. Location of Mongolia in Asia, and the Bugin Tsav locality inside of Mongolia. (World template figure downloaded from Paleobiology Database on April 23 2011.)

MATERIALS AND METHODS

BONE HISTOLOGY: Bone thin sections were created from three specimens: IGM 90/27 posterior portion of articulated carapace and plastron, IGM 90/42 articulated carapace-plastron, IGM 90/28 right costal 6. Procedures follow those described by Schweitzer et al. (2008) and Cadena and Schweitzer (2012), briefly summarized here: bone was embedded in Silmar resin (Surf Source, Atlantic Beach, Florida) sectioning to 1.5 mm slides, ground to a thickness between 60–150 μm (below this range generally the osteocytes are lost, leaving just the empty lacuna), polishing, and final examination using Zeiss Axioskop 2 plus biological microscope and a Zeiss Axioskop 40 petrographic polarizing microscope. Images were taken using Axiovision software package (version 4.7).

OSTEOCYTE VOLUME: Volumetric osteocyte density (VOD), defined as the number of osteocytes per unit of area divided by the thickness of the bone thin section was measured in three randomly selected fields for each of the three different bone tissues of the shell (external cortex, cancellous bone, and internal cortex). VOD was calculated from the bone thin section images using the cell counter and area calculator in ImageJ 1.44o (Abramoff et al., 2004). The

area calculator was calibrated against the bar scale established by the Axiovision software according to the objective lens magnification used. Empty volume due to porosity was calculated and then subtracted from the total volume. The three values of VOD calculated for each of the three tissue types were averaged and then log-transformed to reduce the positive skew of the density distribution.

SYSTEMATICS

Testudines Batsch, 1788

Cryptodira Gradzinski et al., 1977

Lindholmemydidae Chkhikvadze, in Shuvalov and Chkhikvadze, 1975

Mongolemys Khosatzky and Mlynarski, 1971

Mongolemys elegans Khosatzky and Mlynarski, 1971

TYPE MATERIAL: *Mongolemys elegans* ZIN. N° RN, T/M-46.1, complete shell of a large specimen (Khosatzky and Mlynarski, 1971: 131, figs 2–4). See table 1 for measurements of this and other specimens referred in this study.

DISTRIBUTION: Upper Cretaceous Nemegt Formation of the Gobi Desert, Mongolia. The precise age of the Nemegt Formation is not well constrained, but is considered to be late Campanian–early Maastrichtian (Gradzinski et al., 1977; Jerzykiewicz and Russell, 1991, Jerzykiewicz, 2000). The new specimens described in this paper were collected from sandstone deposits of the Nemegt Formation at the Bugin Tsav locality in Ömnögov Aimag, Mongolia. The greater Bugin Tsav locality has also yielded previously described specimens of *Mongolochelys efremovi* Khosatzky (1997) and trionychid turtles (Suzuki and Narmandakh, 2004).

REFERRED SPECIMENS: Z. Pal. N°. MgCh/21, nearly complete plastron (Khosatzky and Mlynarski, 1971), Z. Pal. N°. MgCh/57, fragment of anterior lobe of the plastron (Khosatzky and Mlynarski, 1971), Z. Pal. N°. MgCh/27, skull (Khosatzky and Mlynarski, 1971), uncataloged specimen figured in Suzuki and Narmandakh (2004: fig. 5), which we abbreviate here as Specimen A. New specimens described here: IGM 90/11, partial skull and lower jaw, complete carapace and plastron, left tibia, left fibula, right humerus, and right femur from a single individual, IGM 90/27 partial articulated shell, IGM 90/30 articulated shell, IGM 90/22–23 two associated articulated shells, IGM 90/31 nearly complete plastron, IGM 90/51 complete carapace, IGM 90/54 partially preserved carapace, IGM 90/41 complete right hyoplastron; IGM 90/55, partial skull preserving most of the pterygoid and parietal regions.

REVISED DIAGNOSIS: *Mongolemys elegans* is assigned to Lindholmemydidae based on the presence of three or four well-developed inframarginal scales and presence of contacts between the axillary and inguinal buttresses and the costals (also present in geoemydids and some emydids among cryptodires). *Mongolemys elegans* is diagnosed by the following unique combination of characters: (1) very small antrum postoticum; (2) postorbital-squamosal contact; (3) small trochlear process without contribution of parietal; (4) reduced prefrontals on dorsal surface, lacking medial contact; (5) contribution of the pterygoid to the formation of the foramen palatinum posterius; (6) oval fenestra at the contact between the pterygoid and the basisphenoid; (7) axillary

TABLE 1. Measurements (in mm) of *Mongolemys elegans* specimens described in this study.

Specimen	Length as preserved	Width as preserved	Maximum estimated length	Maximum estimated width
IGM 90/11 skull	45	27	57	43
IGM 90/11 carapace	220	180	220	180
IGM 90/11 plastron	190	130	190	130
IGM 90/55 skull	23	14	30	21
IGM 90/27 carapace	110	70	350	300
IGM 90/30 carapace	62	53	73	60
IGM 90/22 carapace	63	56	75	62
IGM 90/23 carapace	39	28	44	32
IGM 90/31 plastron	91	59	91	70
IGM 90/51 carapace	62	53	65	55
IGM 90/54 carapace	46	38	65	52
IGM 90/41 right hypoplastron	40	32	40	32

buttress reaching 1/3 length of costal 1; (8) three inframarginal scales, which do not overlap peripherals; (9), vertebral 1 reaching the posteromedial portion of peripheral 1.

REMARKS: The revised diagnosis defined above is based on the original description by Khosatzky and Młynarski (1971), later observations made by Danilov (1999a, 2003) and this study.

DESCRIPTION AND COMPARISONS

SKULLS

The most complete new specimen described here is IGM 90/11 (fig. 2A–J), which included both a nearly complete, articulated skull and most of the postcranial skeleton of an adult individual. Most of the posterior elements of the cranium are lost and the edges of bones are slightly broken, but the sutural contacts between bones are clearly visible. The skull is slightly crushed toward the left. In general aspect the skull has large orbits facing outward and upward and deep temporal and cheek emarginations. An isolated portion of the cranium preserves most of the quadrate, otic region bones, and the squamosal (fig. 3A–C). IGM 90/55 (fig. 4A–D) represents a partial skull, preserving most of the basicranium and the parietals. Comparisons are made with the two skulls of *Mongolemys elegans* previously described (Khosatzky and Młynarski, 1971; Sukhanov, 2000), as well as with other fossil and extant cryptodires.

The prefrontals of IGM 90/11 lack a midline contact, which is precluded by the long and narrow anterior processes of the frontals. This condition was already noted for *Mongolemys elegans* (PIN 4693) (Sukhanov, 2000: fig. 17.30A), and is also present in some early Cretaceous eucryptodires including *Sinemys gamera* Brinkman and Peng, 1993, *Ordosemys liaoxiensis* Ji, 1995, *Ordosemys brinkmania* Danilov and Parham, 2007, and *Manchurochelys manchoukuoensis* Endo and Shikama, 1942. In contrast, all extant cryptodires have a midline contact between prefrontals.

The left frontal is slightly broken at the orbit margin, but from the right frontal it is evident that the frontal makes up part of the orbit margin, as reported in specimen PIN 4693 (Sukha-

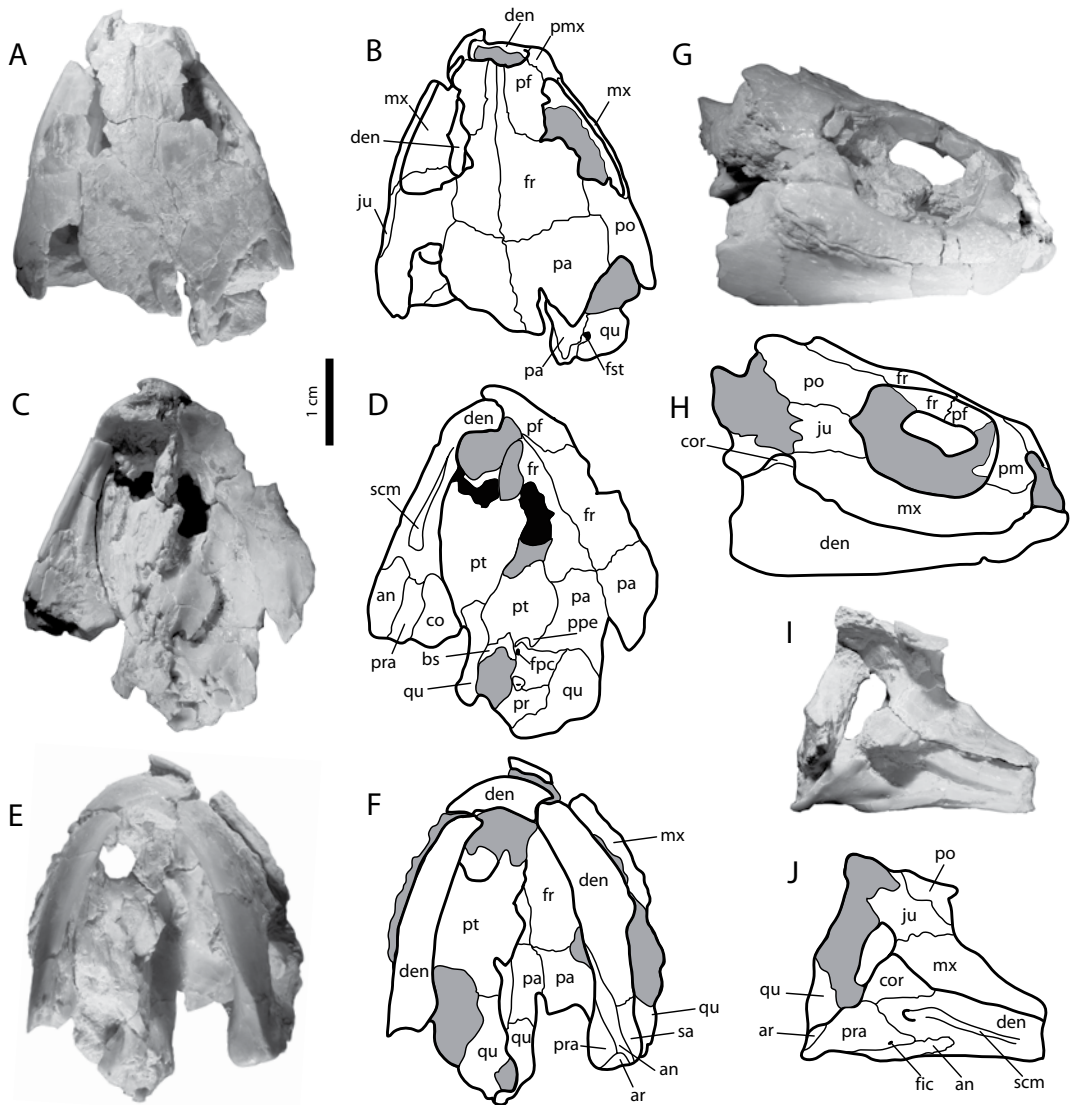


FIG. 2. *Mongolemys elegans* paratype IGM 90/11, skull (cranium and lower jaw): **A–B**, dorsal view; **C–D**, ventrolateral view, removing the left ramus; **E–F**, ventral view, with the left ramus in place; **G–H**, lateral view; **I–J**, medial view of the left ramus and quadrate. Abbreviations: **an**, angular; **ar**, articular; **bs**, basisphenoid; **cor**, coronoid; **den**, dentary; **fpc**, foramen posterius canalis carotici; **fr**, frontal; **fst**, foramen stapedium temporalis; **ju**, jugal; **mx**, maxilla; **pa**, parietal; **pf**, prefrontal; **pmx**, premaxilla; **po**, postorbital; **ppe**, processus pterygoideus externus; **pra**, prearticular; **pt**, pterygoid; **qu**, quadrate; **sa**, surangular; **scm**, sulcus cartilagineus meckelii.

nov, 2000: fig. 17.30A) and observed in most other cryptodires. See Joyce (2007: 11) for discussion of the frontal morphology in other Testudines.

Both parietals are completely preserved anteriorly at the contact with the frontals in IGM 90/11. The right parietal preserves the original lateral margin, indicating that the temporal emargination is very advanced anteriorly, leaving the otic chamber uncovered by the absence of a

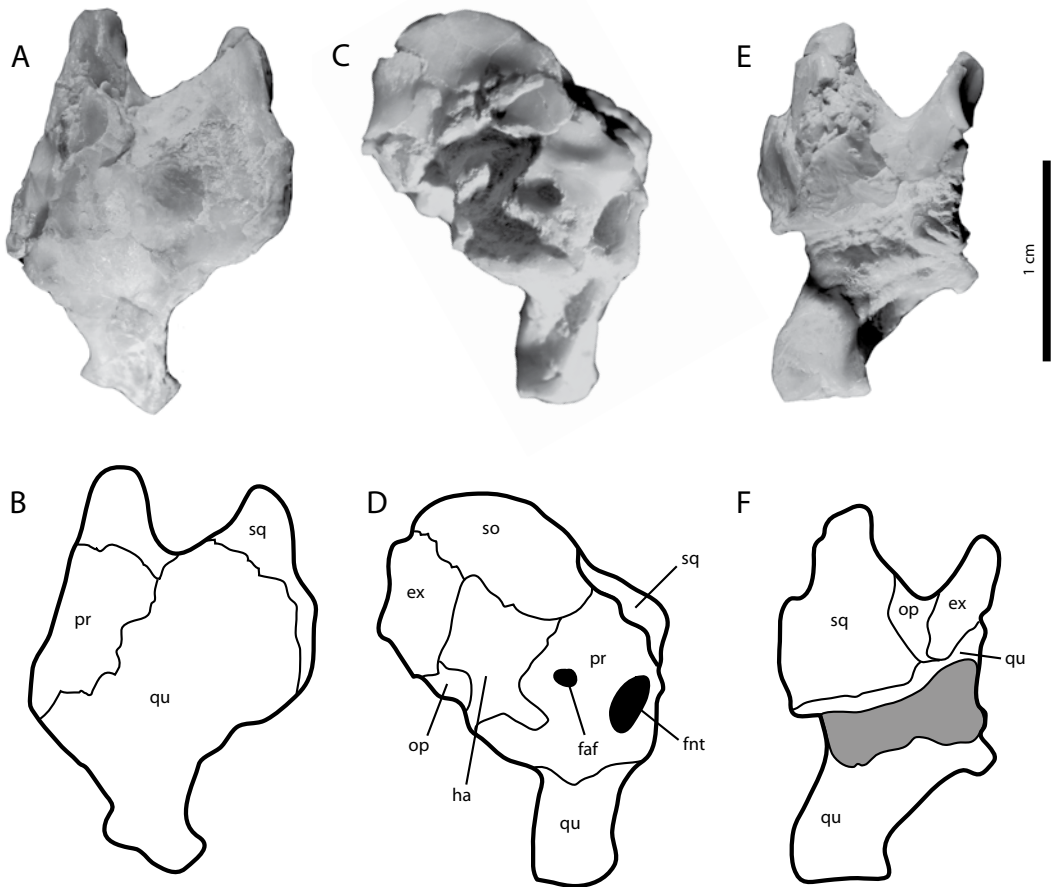


FIG. 3. *Mongolemys elegans* paratype IGM 90/11, isolated left otic chamber-quadrate: **A–B**, anterior view; **C–D**, medial view; **E–F**, posterior view. Abbreviations: **ex**, exoccipital; **faf**, fossa acustico-facialis; **fnt**, foramen nervi trigemini; **ha**, hiatus acousticus; **op**, opisthotic; **pr**, prootic; **qu**, quadrate; **sa**, surangular; **scm**, sulcus cartilaginous meckelii; **so**, supraoccipital; **sq**, squamosal.

parietal roof. This seems to also be the condition for the other two skulls of *M. elegans* previously described in the literature (Khosatzky and Młynarski, 1971; Sukhanov, 2000), and IGM 90/55.

The postorbitals are in medial contact with the frontals and parietals, and ventrolaterally with the jugals. The posterior end of both postorbitals is lost, but based on the marked posterior extension a potential contact with the squamosal is likely, as mentioned by Sukhanov (2000) for specimen PIN 4693.

A small portion of the right quadrate is visible in dorsal view at its contact with the most ventrolateral margin of the parietal, as in specimen PIN 4693, IGM 90/55, and some testudinoids, particularly the geoemydids *Cuora amboinensis* Daudin, 1802, *Rhinoclemmys pulcherrima* Gray, 1855, *Rhinoclemmys areolata* Duméril et al., 1851, *Rhinoclemmys funereal* Cope, 1875, *Rhinoclemmys puntularia* Daudin, 1802, *Rhinoclemmys rubida* Cope, 1870, and *Geocle-*

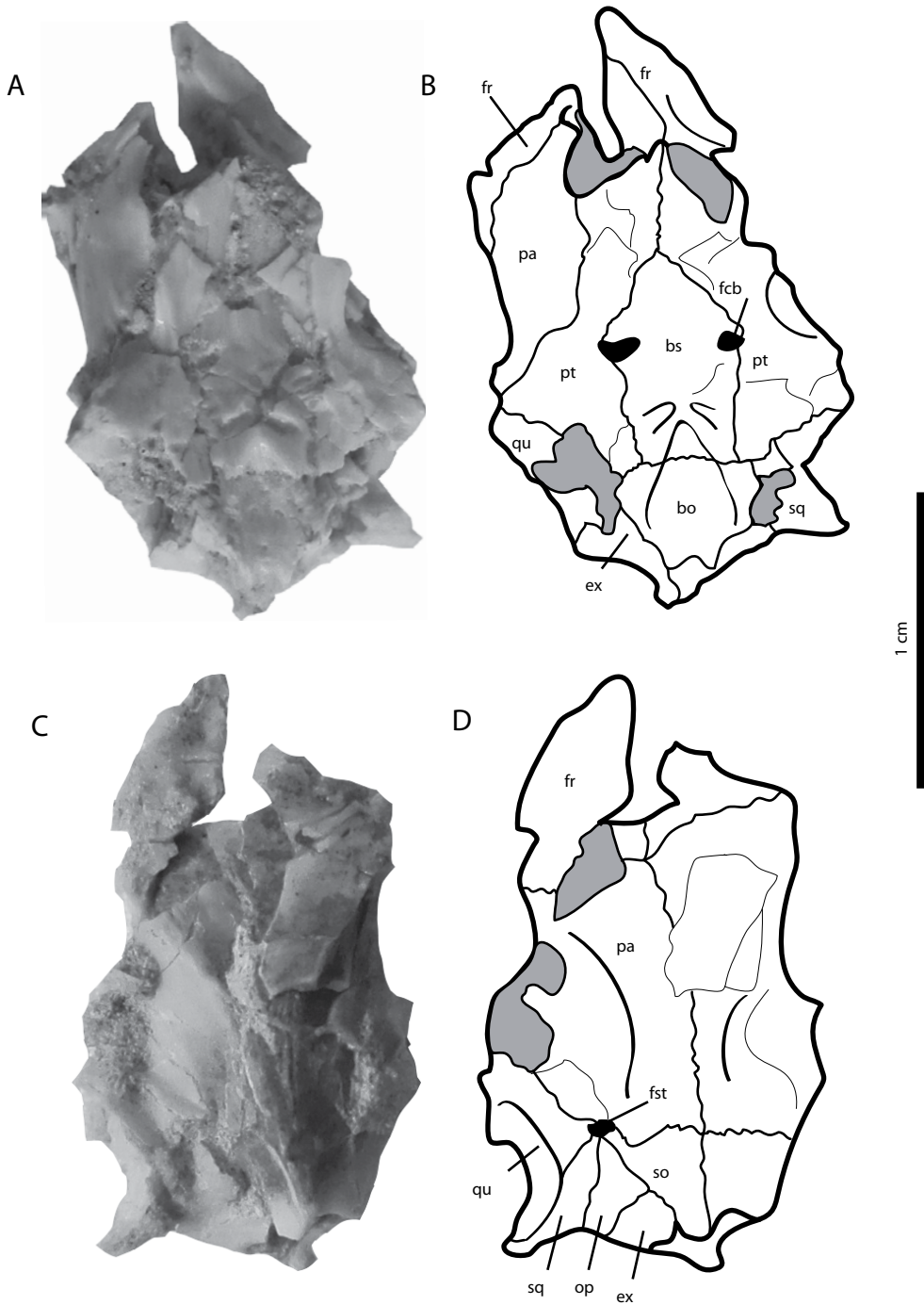


FIG. 4. *Mongolemys elegans* IGM 90/55, partially preserved skull. A–B, ventral view; C–D, dorsal view. Abbreviations in addition to those in figures 2 and 3: fbs, foramen caroticum basiphenoideale.

mys hamiltonii Gray, 1831, and the trionychid *Trionyx triunguis* Forskal, 1775. The foramen stapedio-temporale is located at the suture between the quadrate and the parietal (as observed in specimen PIN 4693 and IGM 90/55) as a result of a highly reduced dorsal exposure of the prootic, a condition common in testudinoids. On the ventral surface of IGM 90/11, small portions of the right quadrate are visible in two different regions: at its dorsomedial contact with the parietal and at the anteroventral contact with the pterygoid. The most ventral portion of the left quadrate is articulated to the left ramus of the lower jaw and preserved in separation from the rest of the skull (fig. 2I–J). The left otic chamber including most of the quadrate, squamosal, prootic, exoccipital, opisthotic, and supraoccipital is preserved as an isolated element from the skull (fig. 3A–F). Medially, the prootic clearly preserves the foramen nervi trigemini and the fossa acustico-facialis. The hiatus acusticus is large, located between the opisthotic, exoccipital, supraoccipital, and the prootic. The processus articularis of the quadrate is long, projected ventrally as in specimen PIN 4693 and all other cryptodires.

Both pterygoids are partially preserved in IGM 90/11, but highly crushed. The left pterygoid preserves the foramen posterius canalis carotici interni, as well as the processus pterygoideus externus, which is very short, as in all testudinoids. A very small portion of the basisphenoid and the prootic are also visible on the ventral surface. IGM 90/55 preserves most of the posteriomedial portions of both pterygoids, which contact the basioccipital posteriorly and the parietals and quadrate laterally. The basisphenoid has a pentagonal shape, exhibiting a small foramen carotium basisphenoidale at the lateral sutural contact with the pterygoid, which is also present in the specimen PIN 4693. In the stem cryptodires *Sinemys lens* Wiman, 1930, and Xinjinagchelyidae, the foramen carotium basisphenoidale makes part of large fossa located between the basiphenoid-ptyerygoid sutural contact (see Kear and Lee, 2006: char. 36). All testudinoids lack a ventral expression of the foramen carotium basiphenoidale at the basisphenoid-ptyerygoid contact.

LOWER JAW

The lower jaw of IGM 90/11 is preserved in articulation with the cranium. On the dentary the sulcus cartilaginis meckelii is deep and ends posteriorly with the opening for the foramen intermandibularis medius. Both dentaries are fused at the symphysis, and the angle between the rami is around 60°. In medial view (fig. 2I–J) the coronoid is very high due in part to crushing. The foramen intermandibularis caudalis is visible in the prearticular, located very close to the suture with the angular. The area of the triturating surface that is visible in dorsomedial view is smooth and very narrow, lacking ridges or toothlike processes. In all of these aspects it resembles the lower jaw of geoemydids and some emydids (e.g., *Glyptemys muhlenbergii*, specimen UF 85274). In other emydids (e.g., *Trachemys scripta*, observed in NCSM 74304 and 74305), the triturating surface is wide with elongate shallow fossae. In the dermatemydid *Dermatemys mawii* (observed in USNM 66669), the triturating surface is very wide with strong toothlike processes.

CARAPACE

IGM 90/11 (fig. 5A–D) includes a nearly complete shell (articulated carapace and plastron). The carapace lacks only some of the left anterior peripherals and some portions of the costals.

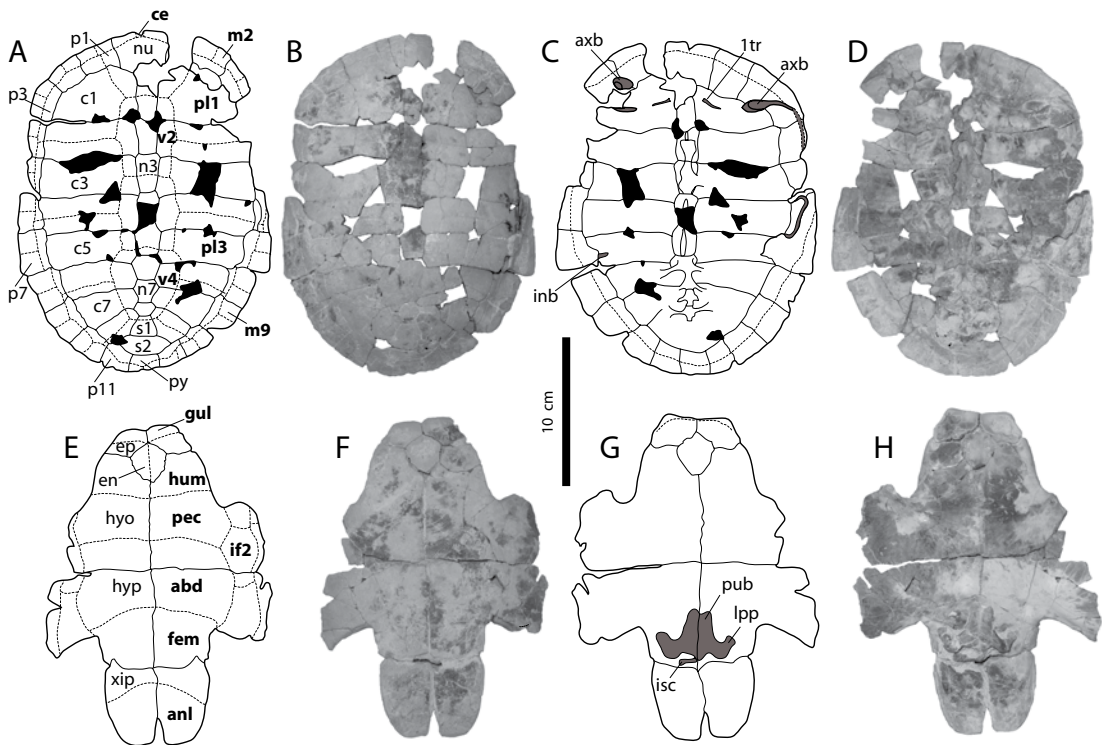


FIG. 5. *Mongolemys elegans* paratype IGM 90/11, articulated shell (carapace and plastron): A–B, carapace, dorsal view; C–D, carapace, ventral view; E–F, plastron, ventral view; G–H, plastron, dorsal view. Abbreviations: **abd**, abdominal scale; **anl**, anal scale; **axb**, axillary buttress; **c**, costal; **ce**, cervical scale; **en**, entoplastron; **ep**, epiplastron; **fem**, femoral scale; **gul**, gular scale; **hum**, humeral scale; **hyo**, hyoplastron; **hyp**, hypoplastron; **if**, inframarginal scale; **ing**, inguinal buttress; **isc**, ischium; **lpp**, anal scale **m**, marginal scale; **n**, neural; **p**, peripheral; **pl**, pleural scale; **pub**, pubis; **py**, pygal scale; **s**, suprapygals. Missing portions of bone in black, scales in dotted lines. Labels in bold indicate scales.

There is no evidence of general crushing, indicating the shell had a moderately domed shape as in the holotype of *Mongolemys elegans*. The size of the carapace (22 cm long, 17.5 cm wide, 7 mm average thickness) indicates a potential subadult individual. There are no keels and the sculpturing of the dorsal surface is principally branching sulci.

The nuchal has a convex anterior edge as in the holotype and the specimen figured by Danilov et al. (2002: fig. 1). It lacks a nuchal emargination, which is present but variably developed in other lindholmemydids (Danilov, 1999a). The holotype of *M. elegans* and the holotype of *Haichemys ulensis*, figured by Sukhanov and Narmandakh (2006: fig. 2), share a nuchal with nearly parallel lateral margins. This feature was one of the putative diagnostic characters used by Sukhanov and Narmandakh (2006) to define the family Haichemydidae, which includes only the species *H. ulensis*. There are eight neurals in IGM 90/11. The neurals exhibit the formula (number of sides) 4-6-6-6-6-6-6-6, as in all other lindholmemydids and *H. ulensis*. Suprapygals 1 is trapezoidal in shape, tapering anteriorly. Suprapygals 2 is hexagonal and very elongated. Eight pairs of costals (completely separated medially by the neurals and the suprapygals), 11

pairs of peripherals, and the pygal together complete the carapace, as in all other lindholmemydids, and most other cryptodires. The cervical scale is very small, rectangular in shape, and slightly smaller than in ZIN. N° RN, T/M-46.1 (*M. elegans* holotype), and other lindholmemydids. Vertebral scale 1 is the widest of the five vertebral scales, pentagonal in shape, and slightly wider than long. Laterally it covers the most posteromedial portion of peripheral 1, as in the holotype and specimen figured by Danilov (2001). This characteristic is exclusive of *M. elegans* within lindholmemydids, and is also present in *H. ulensis*. In all other lindholmemydids and testudinoids vertebral 1 does not cover peripheral 1. The most posterior margin of vertebral 4 reaches the suprapygal 1, which in the holotype and all other lindholmemydids ends over neural 8. Four pairs of pleural scales and twelve pairs of marginals complete the scales covering the bony carapace. The contact between pleural and marginals occurs over the peripherals, as in the holotype and all other lindholmemydids. In testudinoids the pleuro-marginal contact generally overlaps the sutural contact between the costals and peripherals.

On the ventral surface of the carapace, the axillary and the inguinal buttresses and their scars on the costals are well preserved, but weakly developed. The right axillary buttress is out of its original position and placed over the sutural contact between peripheral 1 and 2. The left axillary buttress is still in its original position, indicating a weak development onto costal 1, only reaching about 1/3 of its total length. The development and projection of the axillary buttress onto costal 1 has been used for differentiation within lindholmemydid genera (Danilov, 1999a) defined three different states: (1) weakly developed (1/3 of the costal length) for *Mongolemys elegans*, (2) moderately developed (1/2 of the costal length) for *Gravemys* and *Khodzhakulemys*, and (3) strongly developed (2/3 of the costal length) for *Lindholmemyds* and *Hongilemys*. The inguinal buttress in IGM 90/11 is weakly developed and restricted to costal 5. Variation is seen in the holotype: on the left side the inguinal buttress is restricted to costal 5, but on the right side the inguinal buttress is located between costal 5 and 6. The former condition is present in *Gravemys barsboldi* (Danilov, 2003), and in most testudinoids, with some exceptions as for example *Chinemys reevesi* figured in Joyce and Bell (2004: fig. 110). An inguinal buttress contacting costals 5 and 6 was mentioned by Claude and Tong (2004) as a diagnostic character of Lindholmemydidae. However, based on the new specimens described here, it is clear that there is variation even within individuals and that the most common state in lindholmemydids, as in testudinoids, is an inguinal buttress restricted to costal 5. At the medial region of costal 1, thoracic rib 1 is clearly defined, and resembles the condition for *M. elegans* figured in (Danilov et al., 2002: fig. 2). The last two thoracic vertebrae and the first two sacrals are visible, and exhibit a relative flat dorsal surface and short lateral ribs. The contact between the marginals and the visceral surface is clearly defined for the entire carapace, and corresponds to a shallow sulcus which deepens slightly at the anterior portion of the carapace, as in the holotype.

PLASTRON

The plastron of IGM 90/11 (fig. 5E–H) is nearly complete, missing only the lateralmost portion of the right hyoplastron. The anterior lobe is wider than long, the posterior lobe is longer than wide, and the bridge is longer than either lobe. In all of these aspects the plastron

resembles that of the holotype of *M. elegans* and Specimen A. The anterior lobe has a nearly straight anterolateral margin, same as in the holotype and also in *Gravemys barsboldi*, *G. hutchisoni*, and *Elkemys australis* (Danilov, 2003; Danilov et al., 2012), these three having a shorter anterior lobe. In contrast, *Hongilemys kurzanovi* (Sukhanov, 2000) has a rounded anterior lobe margin. The anteriormost portion of the plastron is unknown for *Lindholmemydids elegans*, *L. martinsoni*, and *Amuremys planicostata*. The posterior lobe in IGM 90/11 has a slightly rounded posterior edge and lacks an anal notch, as in the holotype, Specimen A, and *Lindholmemydids elegans*. In contrast, *G. hutchisoni*, *G. barsboldi*, and *E. australis* have a tapering posterior lobe, with a deep V-shaped anal notch. The posterior lobe is unknown for *A. planicostata* and *L. martinsoni*, and partially preserved anteriorly for *Ho. kurzanovi*. The presence of an anal notch has been considered apomorphic for Testudinoidea (Claude and Tong, 2004; Joyce, 2007). However, the absence of an anal notch in the lindholmemydids mentioned above and the presence of an anal notch in the lindholmemydids *Gravemys* spp. and *Elkemys australis* (see next paragraph) together indicate that presence/absence of this feature cannot be reliably used to separate lindholmemydids from testudinoids.

IGM 90/11 preserves all the plastral scales. The gulars are transversely elongated and contact just the anteriormost corner of the entoplastron as in the holotype, Specimen A, and *Ho. kurzanovi*. The gulars of *Gravemys* spp. and “*Mongolemys*” *trufanensis*, figured by Danilov (2003: fig. 6), cover the anteriormost portion of the entoplastron. This is also the condition in most testudinoids, with some exceptions as, for example, *Rhinoclemmys punctularia* (observed in specimens CRI 2871, 2702, and 2514). As in all other lindholmemydids and extant testudinoids the humeropectoral sulcus does not reach the entoplastron. The pectoral scales are slightly smaller than the abdominals, but not so marked as in all other lindholmemydids. The length of the femorals at midline is slightly longer than that of the anals as in the holotype and Specimen A, whereas the femorals are much longer than the anals in all other lindholmemydids. Within testudinoids this character is variable, and in some cases proportions between right and left femoral/anal scales can be very different within a single individual, as observed in *Trachemys scripta* (specimens NCSM 74304 and 74308). Three inframarginal scales are present and restricted to the hyoplastron and hypoplastron as in the holotype and Specimen A, a characteristic that is exclusive of *Mongolemys elegans* within lindholmemydids (Danilov, 2003). In all other lindholmemydids the inframarginals extend to overlap the peripherals and, in the particular case of *Gravemys* spp., “*Mongolemys*” *trufanensis*, *Paragravemys erratica*, and *Elkemys australis* there are four inframarginals. In IGM 90/11, as in the holotype and Specimen A, the inframarginal 2 is hexagonal in shape, slightly larger than inframarginal 1, and much shorter than inframarginal 3.

On the dorsal surface of the plastron, both pubes are preserved in place, showing a long medial contact between each other and a lateral pubic process, which is ventrolaterally projected, and located far behind the anteriormost tip of the bone. In all these aspects the pubis resembles that of most freshwater testudinoids. A small fragment of the left ischium is preserved and vertically oriented, but no additional features can be described for this bone. Both epiplastra have very incipient epiplastral lips, in contrast to almost all testudinoids which have very thick and marked epiplastral lips.

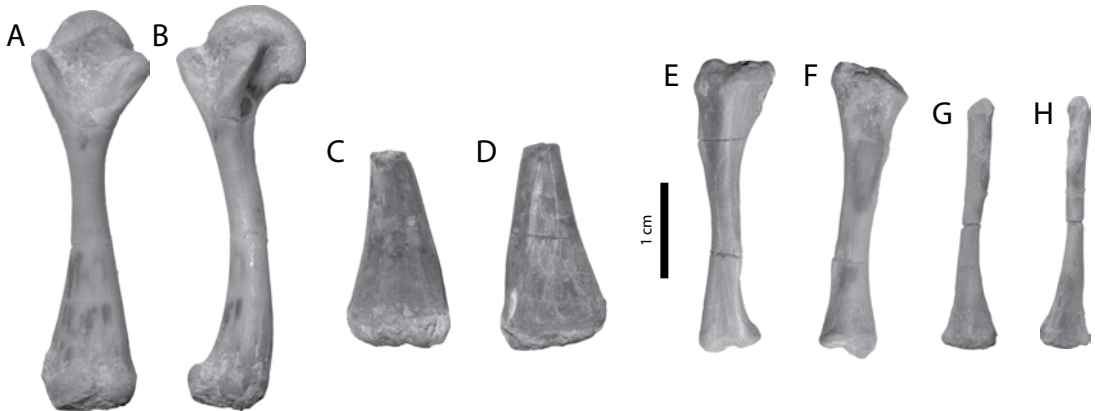


FIG. 6. *Mongolemys elegans* paratype IGM 90/11, long bones. Left femur: **A**, ventral view; **B**, posterior. Right humerus: **C**, ventral view; **D**, dorsal view. Left tibia: **E**, dorsal view; **F**, ventral view. Left fibula: **G**, dorsal view; **H**, ventral view.

LONG BONES

Four long bones were found inside the rock sediments that were infilling the shell of IGM 90/11, including a partial right humerus, left femur, left tibia, and left fibula (fig. 6A–H). The distal end and approximately 20% of the diaphysis of the right humerus is preserved, including the ectepicondylar foramen. In ventral view the capitulum and trochlea are medially positioned. The left femur is completely preserved, as well as the left tibia and left fibula. In all aspects the forelimb and hind-limb bones of *M. elegans* IGM 90/11 resemble those of freshwater testudinoids, and other freshwater turtles in general (e.g., podocnemidids).

ADDITIONAL REFERRED MATERIAL

Multiple specimens from the same locality as for IGM 90/11 exhibit the diagnostic characteristics of *Mongolemys elegans* mentioned above, and reveal additional features of the morphology and ontogeny of *M. elegans*.

IGM 90/27 (fig. 7A–E) corresponds to the right posterolateral portion of an articulated shell and exhibits strong crushing. Based on the size as preserved the shell of this specimen was much larger than IGM 90/11, probably reaching 30 cm total length at midline (see table 1 for measurements). Features including pleuro-marginal sulcus restricted to peripherals, inguinal buttress weakly developed onto costal 5, and the three inframarginals restricted to the hyoplastron and the hyoplastron support referral to *M. elegans*. The microsculpture of interdigitated sulci is excellently preserved in this specimen (fig. 7E). A small region of the posterior portion of this specimen was used to study the bone histology of adult *M. elegans* individuals (see Bone Histology, below).

IGM 90/30 (fig. 8A–D) is a small articulated shell, corresponding to a very young specimen. The posteriormost region of the carapace and the right epiplastron are missing. In all aspects this specimen resembles IGM 90/30, holotype, and Specimen A with the exception of

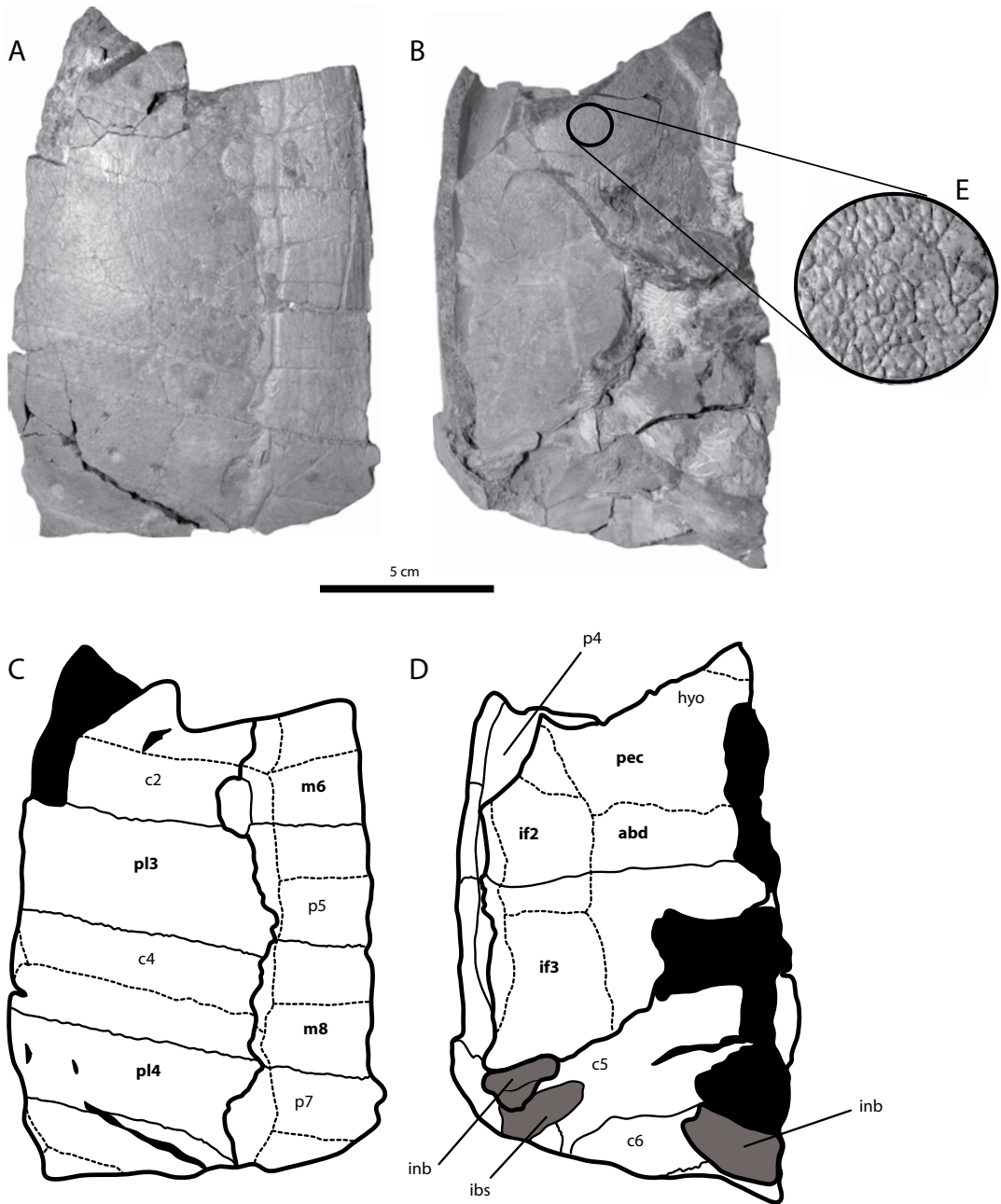


FIG. 7. *Mongolemys elegans* IGM 90/12, posterolateral portion of an articulated adult shell: **A, C**, dorsal view; **B, D**, ventral view. **E**, Close up of a small region of the hyoplastron, showing excellent preservation of the microsculptural branchi sulci texture. Abbreviations: see figure 4. Labels in bold indicate scales.

the slight onlap of the gulars over the most anterior portion of the entoplastron, which is, however, much less advanced than in the other lindholmemydids. The posterior margins of the xiphiplastra converge tapering at the midline of the plastron.

IGM 90/22-23 (fig. 8E-F) are two associated articulated shells, one representing a juvenile specimen (IGM 90/22), and the second representing a hatchling that is preserved atop the juvenile, attached by matrix (IGM 90/23). In both carapaces the number and shape of neurals, as well as the position of sulci between scales is consistent with those exhibited by IGM 90/11 and the holotype.

IGM 90/31 (fig. 8G-H) corresponds to a nearly complete plastron of a juvenile specimen. The three inframarginals have the same shape as in the other specimens of *M. elegans* described above; inframarginal 2 is pentagonal in shape. In this specimen the gulars also just reach the anteriormost corner of the entoplastron as in IGM 90/30.

IGM 90/51 (fig. 8I-J) corresponds to a complete carapace of a young juvenile that, in ventral view, preserves the complete series of 10 procoelous caudal vertebrae with strongly developed chevrons, the weakly developed inguinal and axillary buttresses, and the slightly dorsally convex thoracic vertebrae 1-3. Amphicoelous caudal vertebra at the base of the tail were reported by Danilov (2001) in Specimen A attributed to *Mongolemys*.

IGM 90/54 (fig. 8K-L) corresponds to a partially preserved carapace of a hatchling/juvenile specimen. In ventral view the series of thoracic vertebrae 1-6 is clearly delimited, and the ribs project lateroventrally toward the costals. Axillary buttress scars indicate a weak development of this buttress onto costal 1.

IGM 90/41 (fig. 8M-N) corresponds to a complete right hyoplastron from a juvenile specimen. Inframarginal 2 has the pentagonal shape exhibited by the other specimens of *M. elegans* described above. The microsculpture of branching sulci is also well preserved in this specimen.

BONE HISTOLOGY

GENERAL STRUCTURE

For all three ontogenetic stages of *M. elegans*, the bone structure of the carapace has three well differentiated layers or bone tissue types, which have been characterized for very large number of Testudines by Scheyer (2007), Scheyer and Sanchez-Villagra (2007), whose terminology we adopt for the descriptions below. In *M. elegans*, the external and internal cortices are similar in thickness and the cancellous bone layer is the thickest of the three for both the plastron and the carapace.

EXTERNAL CORTEX: The bone surface of the external cortex of juveniles (fig. 9A) is rough, with low vascularization expressed by a low density of widely spaced primary osteons embedded in a matrix of interwoven structural collagenous fiber bundles. Additionally, Sharpey's fibers are very abundant with an almost vertical orientation, indicating the proximity of this costal bone to the next one. In adult stages the external cortex remains rough, exhibits far fewer primary osteons, and shows an increase in the development of reticular bone (fig. 9G, J). In contrast to that of the carapace, the external cortex of the plastron (fig. 9F) exhibits higher levels of vascularization with larger and more abundant primary osteons.

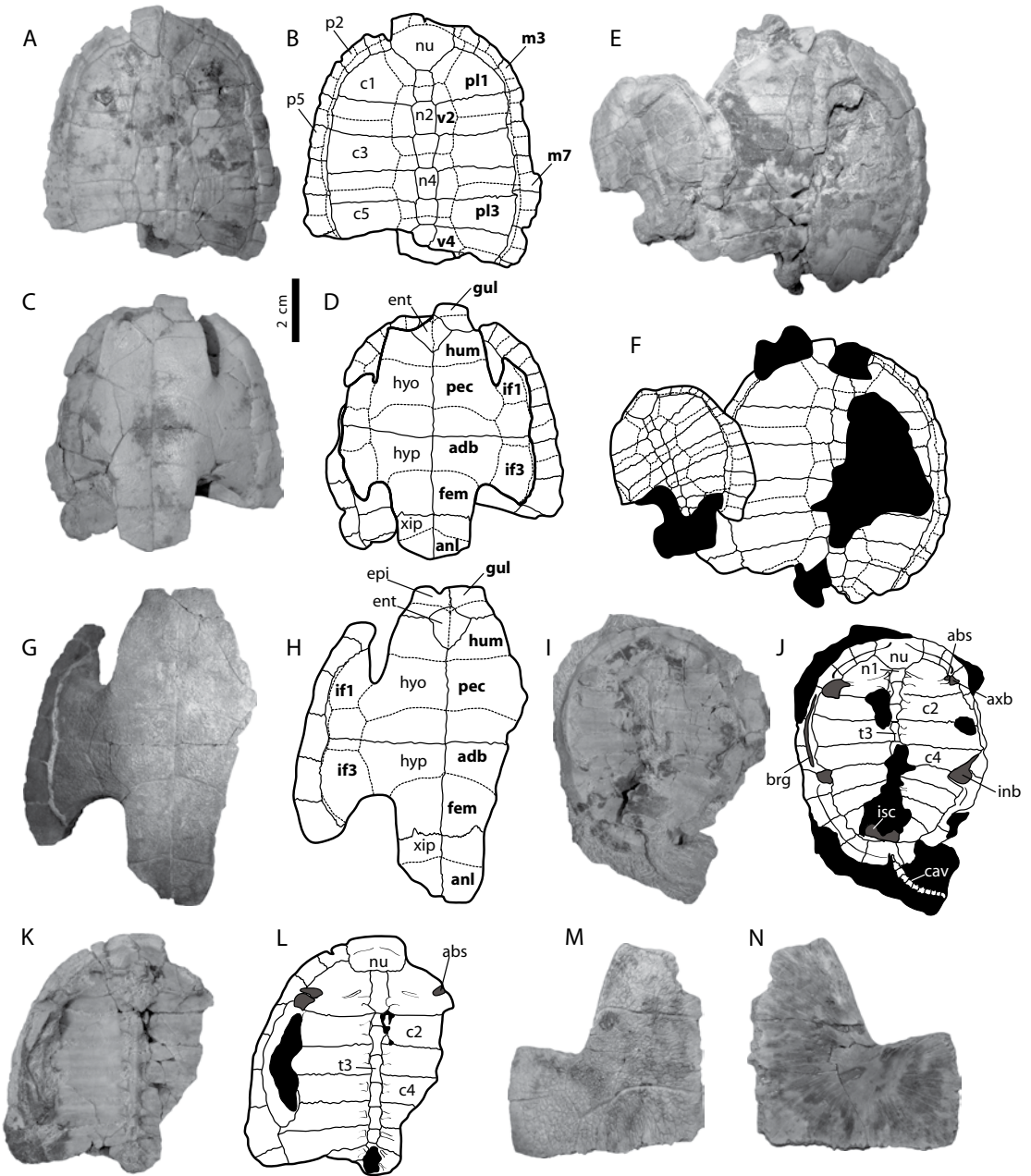


FIG. 8. *Mongolemys elegans*, additional material. IGM 90/30, small articulated shell: A-B, dorsal view; C-D, ventral view. IGM 90/22-23, one juvenile and one hatchling associated shells: E-F, dorsal view. IGM 90/31, nearly complete plastron of a juvenile: G-H, ventral view. IGM 90/51, complete carapace and caudal vertebrae series: I-J, ventral view. IGM 90/54, partial carapace showing the complete series of thoracic vertebrae: K-L, ventral view. IGM 90/41, complete right hyoplastron from a juvenile specimen: M, ventral view; N, dorsal view. Abbreviations: **abs**, axillary buttress scar; **brg**, bridge; **cav**, caudal vertebra. (See fig. 4 for remaining abbreviations).

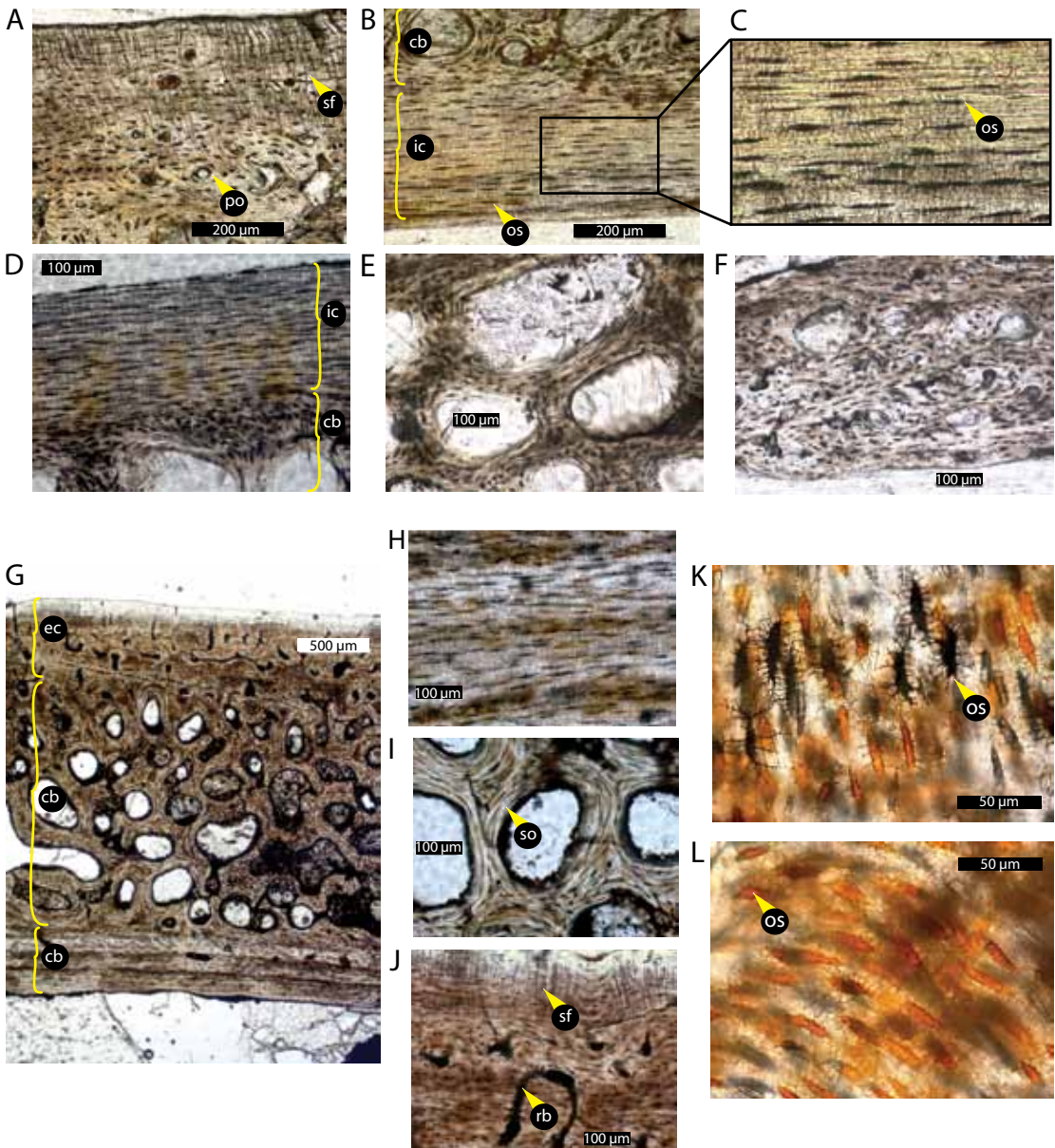


FIG. 9. *Mongolemys elegans*, bone macrostructure and microstructure. Photographs of thin sections, all were taken in transmitted light, 40x otherwise is indicated. IGM 90/42, hatchling-juvenile specimen. **A**, external cortex and part of the cancellous bone of a costal; **B–C**, internal cortex and part of the cancellous bone of a costal; **D**, internal cortex and part of the cancellous bone of the hypoplastron; **E**, cancellous bone of the hypoplastron; **F**, external cortex of the hypoplastron. IGM 90/12, adult specimen. **G**, general view of the costal, showing the external, internal, and cancellous bone layers, photograph take in transmitted light, 10x. **H**, internal cortex of a costal; **I**, cancellous bone of a costal; **J**, external cortex of a costal. **K–L**, osteocytes in the cancellous bone, both taken in transmitted light, 63x oil lens. Abbreviations: **cb**, cancellous bone; **ec**, external cortex; **ic**, internal cortex; **os**, osteocyte; **po**, primary osteon; **rb**, reticular bone; **sf**, Sharpey's fiber; **so**, secondary osteon.

CANCELLOUS BONE: In juveniles the cancellous portion of the shell is highly vascularized, with abundant secondary osteons. These secondary osteons increase in size in adult stages (fig. 9G–I). The secondary osteons in juveniles and adults are composed of an average of seven lamellar bone layers. In the adult stage, the erosion cavities are large, and some of them form elongated channels (filled principally by quartz in this sample). Also in the adult stage at least two generations of secondary osteons are clearly identifiable by cement lines. Cancellous bone layers of the plastron (fig. 9D, E) exhibit the same characteristics described above for the carapace.

INTERNAL CORTEX: The internal cortex is similar in the juvenile and adult stages. It is dominated by avascular parallel-fibered bone (fig. 9B–C). In the adult stage these fibers are slightly rotated relative to one another, creating a succession of light and dark bands (fig. 9G–H) that is characteristic of lamellar bone (Scheyer, 2007). Internal cortex layers of the plastron (fig. 9D) exhibit the same characteristics described above for the carapace.

OSTEOCYTE MORPHOLOGY

Morphological aspects of osteocyte lacuno-cunicular networks, as well as the variations in density of osteocytes per volume of bone and according to bone tissue type, can be characterized for *M. elegans*. Osteocytes in the carapace and plastron of *M. elegans* show exquisite preservation of three-dimensional morphology hitherto unreported for fossil turtles, including the morphology of the main cell bodies as well as the network of channels for the filopodia. In most cases the filopodial channels reach a third level of ramification. Due to differential mineralization, the osteocytes also exhibit a high variety of colors, which include black, brownish, and orange (fig. 9K). The osteocytes located at the internal cortex are particularly elongated and oriented parallel to the lamellar bone. Those located in the large secondary osteons of the cancellous bone are arranged in a concentric way pattern, thus also maintaining an orientation parallel to the lamellar bone layers. Osteocytes in the external cortex are much less elongated than in the internal cortex, and in most cases they are semicircular. In most aspects the relationships of osteocytes to bone layers in *M. elegans* conform to the patterns exhibited by other turtles as recently described by Cadena and Schweitzer (2012).

OSTEOCYTES DENSITY PER VOLUME OF BONE (VOD)

The density per volume of bone (VOD) was calculated for each of the three layers of bone, in both juvenile and adult stages, using the same thin sections described above. The result of the VOS analysis are shown in table 2 and figure 11, the raw data for the analysis including thickness of the bone thin sections used to calculate volume of bone, areas, and osteocyte counts are available in appendix 2.

DISCUSSION

SIMILARITY BETWEEN *MONGOLEMYS ELEGANS* AND *HAICHEMYS ULENSIS*

Haichemys ulensis, the single member of Haichemydidae (Sukhanov, 2000; Sukhanov and Narmandakh, 2006), shares two main apomorphies that diagnose *Mongolemys elegans*: (1)

TABLE 2. Thin sections and their corresponding bone, ontogenetic stage, and VOD (volumetric osteocytes density) for each of the three layers, values given in osteocytes (O) per mm³ of bone.

Thin section	Bone	Ontogenetic stage	VOD EC (O/mm ³)	VOD CB (O/mm ³)	VOD IC (O/mm ³)
IGM 90/12	costal	adult	10138	8701	8212
IGM 90/42	hypoplastron	juvenile	18276	12056	12138
IGM 90/26	costal	hatchling-juvenile	11590	12221	10999

three inframarginal scales, which do not overlap the peripherals, and (2) vertebral 1, which reaches the posteromedial portion of the peripheral 1, causing the nuchal sides to be almost parallel (present in the holotype of *M. elegans*, but variably parallel or subparallel in other specimens). Variation in the inclination of the lateral sides of the nuchal is common among individuals of the same species in testudinoids. Ontogenetic variations occur, with the nuchals slightly more inclined in adults of, for example, *Rhinoclemmys puntularia*. Based on the evidence described above, we consider it most likely that all specimens of *H. ulensis* represent hatchlings of *M. elegans*. However, a conclusive test of the validity of Haichemydidae will be possible only with the discovery of associated skull-shell specimens.

MONGOLEMYS ELEGANS AND THE HIGHER LEVEL AFFINITIES OF LINDHOLMEMYDIDAE

The Lindholmemydids *Mongolemys elegans*, *Gravemys hutchisoni*, *Gravemys barsboldi*, *Hongilemys kurzanovi*, *Lindholmemydids elegans*, *Lindholmemydids martinsoni*, and *Paragravemys erratica* as well as the fossil testudinoids *Palaeoemys hessiaca* Schleich, 1994, *Achilemys cassouleti* Claude and Tong, 2004, and *Pseudochrysemy gobiensis* Sukhanov and Narmandakh, 1976, were added to the character-taxa matrix of Joyce et al. (2011) (see appendix 1).

An initial analysis was run including all taxa and using the same parameters as specified by Joyce et al. (2011): all characters were considered reversible and assigned equal weight, characters (7, 29, 35, 37, 49, 68, 69, 74, 75, 77, 80, 94, 107, 129, 142, and 143) ordered. A heuristic search was performed using PAUP version 4.0a125 (Swofford, 2002) for 1000 replicates, with multistate characters considered polymorphic. A strict consensus of 964,275 most parsimonious trees (fig. 10A) with tree length (TL) = 449, consistency index (CI) = 0.434, retention index (RI) = 0.802, and rescaled consistency index (RC) = 0.384 shows a large polytomy inside Cryptodira involving testudinoids and lindholmemydids.

In the second analysis, we excluded all lindholmemydids except *Mongolemys elegans* and the three fossil testudinoids that lacked associated skull and shell material. All search parameters were the same as for the first analysis. A strict consensus tree was obtained from 270 most parsimonious trees (fig. 10B), with TL = 447, CI = 0.480, RI = 0.798, and RC = 0.382. *Mongolemys elegans* is recovered as pantestudinoid, supporting the attribution made by Danilov and Sukhanov (2001) and the result obtained in the phylogenetic analysis of Sterli (2010). Pantestudinoidea is supported here by the presence of an axillary buttress reaching costal 1 (char. 95), and Testudinoidea is supported by the presence of an weak anal notch (char. 96)

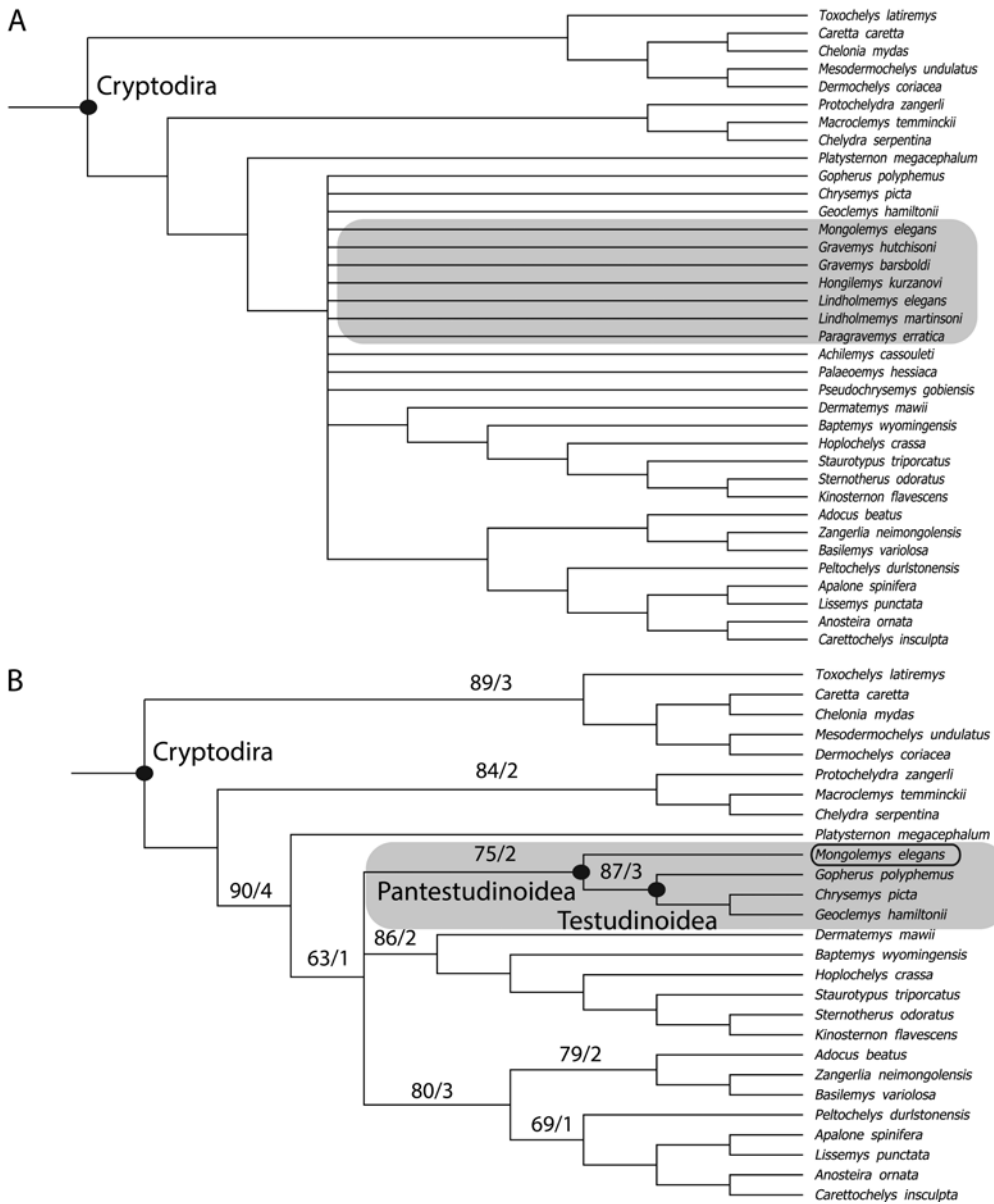


FIG. 10. Phylogenetic hypotheses for the relationship of *Mongolemys elegans* among cryptodires. **A**, strict consensus tree including all characters and taxa as in appendix 1. Taxa outside of Cryptodira were excluded for the purpose of this figure. Tree length (TL): 449, Consistency index (CI): 0.434, Retention index (RI): 0.802, Rescaled index (RC): 0.384. **B**, strict consensus after excluding all lindholmemydids except *Mongolemys elegans* and the three fossil testudinoids (*Palaeoemys hessiaca*, *Achilemys cassouleti* and *Pseudochrysemys gobiensis*). TL = 447, CI = 0.480, RI = 0.798, and RC = 0.382. Bootstrap values from 1000 heuristic search replicates (left) and Bremer support values (right) are provided above or below the branches they pertain too.

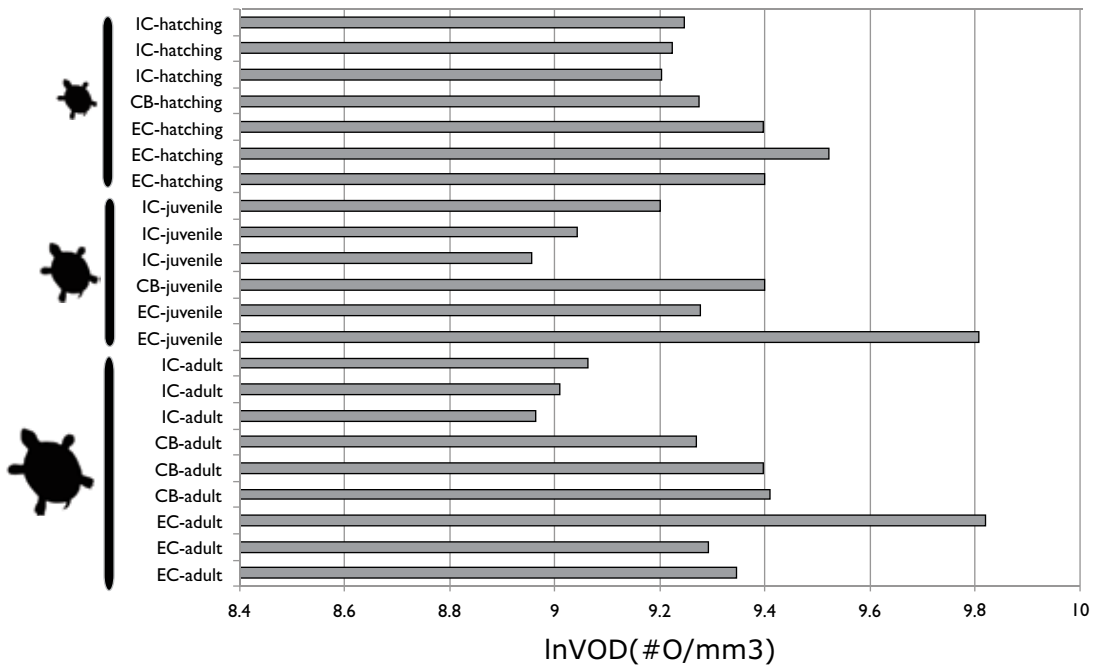


FIG. 11. Type of bone layer vs. log-transformed value for volumetric osteocytes density ($\ln\text{VOD}(\#O/\text{mm}^3)$) for adult, juvenile, and hatching specimens of *Mongolemys elegans*. Abbreviations: **cb**, cancellous bone; **ec**, external cortex; **ic**, internal cortex.

and two pairs of inframarginal restricted to the axillary and inguinal regions, allowing contact between plastral and marginal scales (char. 109).

Our phylogenetic results reaffirm that Lindholmemydidae remains problematic in the context of higher-level turtle phylogeny because all the taxa included in this group, except for *Mongolemys elegans*, lack complete skeletons, which contributes to a lack of resolution in phylogenetic analyses. Although *Mongolemys* is supported as a member of Pantestudinoidea, more work is needed to determine whether Lindholmemydidae is monophyletic. The new material described here actually reveals one previously unrecognized cranial similarity between *M. elegans* and some testudinoids. The presence of a contact between the quadrate and the parietal, which are well exposed dorsally at the roof of the otic chamber and encapsulate the foramen stapedium temporalis, is shared by *M. elegans* and the Geoemydidae (one of the largest groups of Asian testudinoids). In other testudinoids, however, the prootic generally prevents contact between the parietal and quadrate at the dorsal roof of the otic chamber, suggesting this feature may be convergently acquired.

BONE MICROSTRUCTURE IN *MONGOLEMYS ELEGANS*

Bone macrostructure provides additional support for the phylogenetic placement of *Mongolemys elegans*. When this species was originally described by Khosatzky and Mlynarski (1971), it was attributed to Dermatemydidae based on the presence of inframarginal scales.

Bone macrostructure of *D. mawii* and other dermatemydids shows a particular trabecular arrangement in the cancellous bone that is highly organized and apomorphic among turtles (Scheyer, 2007). *M. elegans* lacks the pattern of cancellous bone organization seen in dermatemydids and instead resembles the diploe structure of external-internal cortices and interior cancellous bone of testudinoids, being particularly similar to the Testudinoid histotype III (Scheyer, 2007) that is seen in *Trachemys scripta* as well as geoemydids. The bone macrostructure organization of *M. elegans* shows several features such as similarity in thickness of the external and internal cortices and low vascularization that coincides with ecological category number II of Scheyer (2007), which is typical of semiaquatic to mainly aquatic turtles.

For all three ontogenetic stages studied in *Mongolemys elegans* specimens, the VOD values proved to be higher in the external cortex than in cancellous bone and the internal cortex (fig. 11). Implications of these variations in VOD values for the different cortices and layers of the bone of the turtles is currently under investigation (Cadena, unpubl. data). An important ontogenetic trend in *M. elegans* is the notable reduction in the VOD values for all three layers between hatchling and adult stages. A considerably reduction in osteocyte density with the increase of body mass has been documented in mammals, frogs, lizards, and snakes, with implications for general relationships between of metabolic rate and body mass in vertebrates (Cullinane, 2000). Thus, VOD may be useful in the study of fossil organisms, for example, to aid body-mass estimation of large vertebrates when only fragmentary bones are recovered, to establish variations in metabolic rates in fossil taxa with similar body mass, or even infer changes in metabolic rates during ontogeny or through evolution of a particular lineage. Our data from VOD in *M. elegans* show that turtles also follow the general vertebrate pattern of osteocyte density decreasing over ontogeny.

ACKNOWLEDGMENTS

Funding for the project was provided by a Richard Gilder Graduate School collection study grant from the AMNH. We thank the members of the 1992 Mongolia Academy of Sciences–American Museum of Natural History joint expedition that collected the fossils described here, B. Stuart (NCSM) for access to extant taxa, I. Danilov for providing photos of the holotype of *M. elegans*, T. Cleland and M. Zeng (NCSU) for their help in the preparation of the bone thin sections, and J. Parham and I. Dalinov for helpful comments. For access to collections, we thank P. Pritchard (Chelonian Research Institute), C. Mehling (AMNH), and J. Jacobs (USNM).

REFERENCES

- Abramoff, M.D., P.J. Magelhaes, and S.J. Ram. 2004. Image processing with ImageJ. *Biophotonics International* 11: 36–42.
- Batsch, A.J.G.C. 1788. *Versuch einer Anleitung, zur Kenntniß und Geschichte der Thiere und Mineralien*. Jena: Akademische Buchhandlung, 528 pp

- Brinkman, D.B., and J.H. Peng. 1993. New material of *Sinemys* (Testudines, Sinemydidae) from the Early Cretaceous of China. *Canadian Journal of Earth Sciences* 30: 2139–2152
- Brinkman, D.B., L.A. Nesson, and J.H. Peng. 1993. *Khunnuchelys* gen. nov, a new trionychid (Testudines: Trionychidae) from the Late Cretaceous of Inner Mongolia and Uzbekistan. *Canadian Journal of Earth Sciences* 30: 2214–2223.
- Chkhikvadze, V.M. 1970. Classification of the subclass Testudinata. 16-aja Nauchmaja Sess. Inst. Paleobiol. Akademii nauk Gruzii: 7–8.16th Scientific Session, Institute of Paleobiology, Academy of Sciences, Georgia. [in Russian]
- Cadena, E.A., and M. Schweitzer. 2012. Variation in osteocytes morphology vs bone type in turtle shell and their exceptional preservation from the Jurassic to the present. *Bone* 51 (3): 614–620.
- Claude, J., and H. Tong. 2004. Early Eocene testudinoid turtle from Saint-Papoul, France, with comments on the early evolution of modern Testudinoidea. *Oryctos* 5: 3–45.
- Cope, E. 1870. Seventh contribution to the herpetology of tropical America. *Proceedings of the Academy of Natural Sciences of Philadelphia* 11: 147–149.
- Cope, E. 1875. On the batrachia and reptilia of Costa Rica. *Journal of the Academy of Natural Sciences of Philadelphia* 2: 93–154.
- Cullinane, D. 2000. The role of osteocytes in bone regulation: mineral homeostasis versus mechanoreception. *Journal of Musculoskeletal Neuronal Interaction* 2: 242–244.
- Danilov, I.G. 1999a. A new lindholmemydid genus (Testudines: Lindholmemydidae) from the mid-Cretaceous of Uzbekistan. *Russian Journal of Herpetology* 6 (1): 63–71.
- Danilov, I.G. 1999b. The ecological types of turtles in the Late Cretaceous of Asia. *Proceedings of the Zoological Institute Russian Academy of Sciences* 281: 107–112
- Danilov, I.G. 2001. [Fossil turtles of the family Lindholmemydidae and phylogenetic relationships of cryptodiran turtles]. Ph.D. dissertation, Zoological Institute of the Russian Academy of Sciences, St. Petersburg, 318 p. [in Russian].
- Danilov, I.G. 2003. *Gravemys* Sukhanov and Narmandakh, 1983 (Testudinoidea: Lindholmemydidae) from the Late Cretaceous of Asia: new data. *Paleobios* 23: 9–19.
- Danilov, I.G. 2004. New data on morphology of turtles from the Late Cretaceous of Middle Asia. *Problems of Paleontology of Central Asia. Symposium Abstracts 2004*: 23–25. [in Russian].
- Danilov, I.G., and J.F. Parham. 2005. A reassessment of the referral of an isolated skull from the late Cretaceous of Uzbekistan to the stem-testudinoid turtle genus *Lindholmemys*. *Journal of Vertebrate Paleontology* 4: 784–791.
- Danilov, I.G., and J.F. Parham. 2007. The type series of ‘*Sinemys*’ *wuerhoensis*, a problematic turtle from the Lower Cretaceous of China, includes at least three taxa. *Palaeontology* 50: 431–444.
- Danilov, I.G., and V.B. Sukhanov. 2001. New data on lindholmemydid turtle *Lindholmemys* from the late Cretaceous of Mongolia. *Acta Palaeontologica Polonica* 46: 125–131.
- Danilov, I. G., J. Claude., and V. B. Sukhanov. 2012. A redescription of *Elkemys australis* (Yeh, 1974), a poorly known basal testudinoid turtle from the Paleocene of China. *Proceedings of the Zoological Institute RAS* 316: 223–238.
- Danilov, I.G., Y.L. Bolotsky, A.O. Averianov, and I.V. Donchenko. 2002. A new genus of lindholmemydid turtle (Testudines: Testudinoidea) from the Late Cretaceous of the Amur river region, Russia. *Russian Journal of Herpetology* 9: 155–168.
- Daudin, F.M. 1802. *Histoire naturelle, générale et particuliere des reptiles*. Vol. 2. Paris: F. Dufart, 432 p.
- Duméril, A.M., G. Bibron, and A. Duméril. 1851. *Catalogue méthodique de la collection des reptiles du Museum d’Histoire Naturelle*. Paris: Gide and Boudry, 224 p.

- Endo, R., and T. Shikama. 1942. Mesozoic fauna in the Jehol mountainland, Manchoukuo. *Bulletin of Central National Museum, Manchoukuo* 3: 1–23.
- Forskål, P. 1775. *Descriptiones animalium, avium, amphibiorum, piscium, insectorum, vermium; quae in itinere orientali observavit Petrus Forskål. Hauniaë [Copenhagen]: ex officina Mölleri. 164 p.*
- Gradzinski, R., Z. Kielen-Jaworowska, and T. Maryanóska. 1977. Upper Cretaceous Diadokhta, Barun Govot and Nemegt formation of Mongolia, including remarks on previous subdivisions. *Acta Geologica Polonica* 27: 281–317.
- Gray, J.E. 1831. *Synopsis reptilium, Part I. Cataphracta. Tortoises, Crocodiles, Enaliosauria. London: Treuttel, Wurtz and Co., 85 pp.*
- Gray, J.E. 1847. Description of a new genus of Emydidae. *Proceedings of the Zoological Society of London 1847*: 55–56.
- Gray, J.E. 1855. *Catalogue of shield reptiles in the collection of the British Museum. Part I. Testudinata (Tortoises). London: British Museum, 79 pp.*
- Jerzykiewicz, T. 2000. Lithostratigraphy and sedimentary setting of the Cretaceous dinosaur beds of Mongolia. *In* M.J. Benton (editor), *The age of dinosaurs in Russia and Mongolia*: 279–296. Cambridge: Cambridge University Press, 696 pp.
- Jerzykiewicz, T., and D.A. Russell. 1991. Mesozoic stratigraphy and vertebrates of the Gobi basin. *Cretaceous Research* 12: 345–377.
- Ji, S.A. 1995. Reptiles. *In* D. Ren, L.W. Lu, Z.-G. Guo, and S.-A. Ji (editors), *Faunae and stratigraphy of Jurassic-Cretaceous in Beijing and the adjacent areas*: 140–146. Beijing: Seismic Press.
- Joyce, W.G. 2007. Phylogenetic relationships of Mesozoic turtles. *Bulletin of the Peabody Museum of Natural History* 48: 3–102.
- Joyce, W.G., and C.J. Bell. 2004. A review of the comparative morphology of extant Testudinoid turtles (Reptilia: Testudines). *Asiatic Herpetological Research* 10: 53–109.
- Joyce, W.G., S.D. Chapman, R.T. Moddy, and C.A. Walker. 2011. The skull of the solemydid turtle *Helochelydra nopcsai* from the Early Cretaceous of Isle of Wight (UK) and a review of Solemydidae. *Paleontology* 86: 75–97.
- Kear, B.P., and M.S.Y. Lee. 2006. A primitive protostegid from Australia and early sea turtle evolution. *Biology Letters* 2: 116–119.
- Khosatzky, L.I. 1997. Big turtle of the late Cretaceous of Mongolia. *Russian Journal of Herpetology* 4: 148–154.
- Khosatzky, L.I., and M. Młynarski. 1971. Chelonians from the upper Cretaceous of the Gobi Desert, Mongolia. *Paleontologica Polonica* 25: 131–144.
- Lourenco, J.M., J. Claude, N. Galtier, and Y. Chiari. 2012. Dating cryptodiran nodes: origin and diversification of the turtle superfamily Testudinoidea. *Molecular Phylogenetics and Evolution* 62: 496–507.
- Scheyer, T.M. 2007. Comparative bone histology of the turtle shell (carapace and plastron): implications for turtle systematics, functional morphology and turtle origins. Bonn: Universität Bonn, 125 pp.
- Scheyer, T.M., and M.R. Sanchez-Villagra. 2007. Carapace bone histology in the giant pleurodiran turtle *Stupendemys geographicus*: phylogeny and function. *Acta Palaeontologica Polonica* 52: 137–154.
- Schleich, H.H. 1994. Neu Reptilienfunde aus dem Tertiär Deutschlands. Schildkroten-une Krokodilreste aus der eozanen Braunkohle des Untertagebaus bei Borken (Hessen) (Reptilia: Crocodylia, Testudines). *Courier Forschungsinstitut Senckenberg* 173: 79–101.
- Schweitzer, M., C. Organ, W.X. Zheng, J. Asara, and T. Cleland. 2008. Exceptional preservation of *Brachylophosaurus Canadensis* (Campanian, Judith River Formation, USA). *Journal of Vertebrate Paleontology* 28: 139A.

- Shuvalov, V.F., and V.M. Chkhikvadze. 1975. New data on Late Cretaceous turtles of south Mongolia. *Trudy Sovmestnaia Sovetsko Mongolskaia Geologicheskaiia Ekspeditsii* 2: 209–224.
- Sterli, J. 2010. Phylogenetic relationships among extinct and extant turtles: the position of Pleurodira and the effects of the fossils on rooting crown-group turtles. *Contributions to Zoology* 79: 93–110.
- Sukhanov, V. 2000. Mesozoic turtles of Central Asia. *In* M.J. Benton, M.A. Shishkin, D.M. Unwin, and E.N. Kurochkin (editors.), *The age of dinosaurs in Russia and Mongolia*: 309–367. Cambridge: Cambridge University Press.
- Sukhanov, V.B., and P. Narmandakh. 1976. Paleocene turtles from Mongolia. *Paleontology and biostratigraphy of Mongolia. Joint Soviet-Mongolian Paleontological Expedition Transactions* 3: 107–134.
- Sukhanov, V.B., and P. Narmandakh. 2006. New taxa of Mesozoic turtles from Mongolia. *In* I.G. Danilov and J.F. Parham (editors), *Fossil turtle research*, vol. 1: 119–127. *Proceedings of the Symposium on Turtle Origins, Evolution and Systematics: August 18–20, 2003, St. Petersburg, Russia (Supplement to Russian Journal of Herpetology)*.
- Suzuki, S., and P. Narmandakh. 2004. Change of the Cretaceous turtle faunas in Mongolia. *Hayashibara Museum of Natural Science Research Bulletin* 2: 7–14.
- Sukhanov, V.B., I. Danilov, and P. Narmandakh. 1999. A new lindholmemyid turtle (Testudines: Lindholmemydidae) from the Bayn Shire formation (Late Cretaceous) of Mongolia. *Russian Journal of Herpetology* 6: 147–152.
- Swofford, D.L. 2002. PAUP*. *Phylogenetic analysis using parsimony (*and other methods)*. 4.0 b10. Sunderland, MA: Sinauer Associates.
- Wiman, C. 1930. Fossile Schildkroeten aus China. *Palaeontologia Sinica, Series C* 6 (3): 5–53.
- Yeh H. K. 1994. *Fossil and recent turtles of China*. Beijing: Science Press, 112 pp.

APPENDIX 1

CHARACTER-TAXON MATRIX: ADDITIONS AND CHANGES TO JOYCE ET AL., 2011

To the taxa listed in Joyce et al., we have added: *Mongolemys elegans*, *Gravemys hutchisoni*, *Gravemys barsboldi*, *Hongilemys kurzanovi*, *Lindholmemyd elegans*, *Lindholmemyd martinsoni*, *Paragravemys erratica*, and three fossil testudinoids: *Palaeoemys hessiaca*, *Achilemys cassouleti* and *Pseudochrysemy gobiensis*.

Changes to character list of Joyce et al., 2011

Character 96 (Xiphiplastron A). 0 = absent; 1 = weak; 2 = deep. Comment: one state added, as in Joyce and Bell (2004: char. 61), to cover variations in the depth of the notch.

Changes to the scoring of *Mongolemys elegans* from the matrix of Joyce et al., 2011

Character 4 (prefrontal A): Scoring changed from 0/1 to 0. Our examination of all described skulls of *Mongolemys elegans* documents a lack of a medial contact between prefrontals.

Character 96 (xiphiplastron A): Scoring changed from 1 to 0. All specimens of *Mongolemys elegans* lack an anal notch. Note that the specimen shown in figure 5 has been damaged, creating the appearance of a notch.

Character 123 (dorsal rib B): Scoring of “0” added for *Mongolemys elegans*, based on the new specimens described in this paper which show a contact of dorsal rib 9 and 10 with the costals is present.

Scorings for the taxa added to Joyce et al., 2011, matrix

Mongolemys elegans

1--000111111010000?001200001010022022112110000???21022?0?
1013?01110011001000002111000111000121000001-100000011111?
????01201?1112????01--011????

Gravemys hutchisoni

??
?0011001000002111000111000?21000001-1000000?1????????????
??????0?--????????

Gravemys barsboldi

??
?0011001000002111000111000121100001-1000000????????????20??
??????0?--????????

Hongilemys kurzanovi

??
0011?0?00002111000111000?2?0000011000000????????????????
????????????????

Lindholmemyms elegans

??
0110010000021110001110001210000?1-1?00001????????????????
??0?--????????

Lindholmemyms martinsoni

??
11001000002111000111000122?000?1-1000001????????????20????
0?--????????

Paragravemys erratica

??
1?????????????0?0111000?2?000001-1000000????????????????
??????????

Achilemys cassouleti

??
11001000002111000111000121100001-1000001????????????2????
0?--????????

Palaeoemys hessiaca

??
1001000002111000111000121100001-1000001????????????2????
??????????

Pseudochrysemys gobiensis

??00
 11001000002111000111000?2?100001-1000001????????????????????????????????
 ????????????

APPENDIX 2

RAW DATA FOR THE CALCULATION OF OSTEOCYTE DENSITY PER BONE VOLUME (VOD), USING BONE THIN SECTIONS OF *MONGOLEMYS ELEGANS*

Abbreviations: **CB**, number of osteocytes at the cancellous bone; **EC**, number of osteocytes at the external cortex; **IC**, number of osteocytes at the internal cortex; **VOD**, number of osteocyte/bone volume. Areas and osteocytes counting calculated using ImageJ 1.44o (Abramoff et al., 2004). Area accounted for by VOD = total bone area - total porosity area; thickness of bone thin section was obtained with a precision micrometer; bone volume = area accounted for by VOD * thickness.

Thin section	EC	CB	IC	Total bone (µm ²)	Total porosity (µm ²)	Area accounted for by VOD (µm ²)	Area accounted for by VOD (mm ²)	Thick-ness (mm)	Bone volume (mm ³)	VOD (#/mm ³)
IGM 90/26		301		359242.50	145074.00	214168.50	0.21	0.115	0.02	12221.18
		442		360943.46	42431.45	318512.01	0.32	0.115	0.04	12066.98
		365		366076.63	67121.40	298955.23	0.30	0.115	0.03	10616.68
		415		366078.39	67565.97	298512.42	0.30	0.115	0.03	12088.93
			269	264601.60	45350.69	219250.92	0.22	0.115	0.03	10668.74
			288	272137.84	53639.15	218498.69	0.22	0.115	0.03	11461.61
			228	329639.77	147203.68	182436.09	0.18	0.115	0.02	10867.42
IGM 90/42	409			361176.51	43504.23	317672.28	0.32	0.07	0.02	18392.72
	253			360197.71	161168.78	199028.93	0.20	0.07	0.01	18159.60
			245	358244.02	30828.35	327415.67	0.33	0.07	0.02	10689.78
			170	359773.03	158762.38	201010.65	0.20	0.07	0.01	12081.80
			172	357032.95	176937.94	180095.02	0.18	0.07	0.01	13643.59
		105	163878.77	39460.05	124418.72	0.12	0.07	0.01	12056.06	
IGM 90/12			394	366978.39	7050.55	359927.84	0.36	0.14	0.05	7819.03
			393	366407.19	23442.66	342964.53	0.34	0.14	0.05	8184.94
			424	372079.27	21251.22	350828.05	0.35	0.14	0.05	8632.64
			258	348311.92	110434.45	237877.46	0.24	0.14	0.03	7747.09
			282	365084.94	127031.38	238053.55	0.24	0.14	0.03	8461.48
			314	359778.88	133108.96	226669.92	0.23	0.14	0.03	9894.82
		468		354045.44	17122.70	336922.74	0.34	0.14	0.05	9921.73
		399		342982.21	61618.55	281363.66	0.28	0.14	0.04	10129.24
	427		354423.44	60142.51	294280.94	0.29	0.14	0.04	10364.25	

Complete lists of all issues of *Novitates* and *Bulletin* are available on the web (<http://digitallibrary.amnh.org/dspace>). Inquire about ordering printed copies via e-mail from scipubs@amnh.org or via standard mail from:

American Museum of Natural History—Scientific Publications
Central Park West at 79th Street
New York, NY 10024

Ⓢ This paper meets the requirements of ANSI/NISO Z39.48-1992 (permanence of paper).